Available online at www.sciencedirect.com
SCIENCE DIRECT
Talanta 69 (2006) 1285–1291
Talanta
www.elsevier.com/locate/talanta

A three-dimensionally adjustable amperometric detector for microchip electrophoretic measurement of nitroaromatic pollutants

Xiao Yao [a], Joseph Wang [b], Luyan Zhang [a], Pengyuan Yang [a], Gang Chen [a,*]

[a] *Department of Chemistry, Fudan University, Shanghai 200433, China*
[b] *Departments of Chemical & Materials Engineering and Chemistry, Arizona State University, Tempe, AZ 85287-5001, USA*

Received 20 October 2005; received in revised form 30 December 2005; accepted 6 January 2006
Available online 7 February 2006

Abstract

A microchip capillary electrophoresis (CE)–amperometric detection (AD) system has been fabricated by integrating a two-dimensionally adjustable CE microchip and an amperometric detection cell containing a one-dimensionally adjustable disc detection electrode in a Plexiglas holder. It facilitates the precise three-dimensional alignment between the channel outlet and the detection electrode without a complicated three-dimensional manipulator. The performance of this unique system was demonstrated by separating four nitroaromatic pollutants (nitrobenzene, 2,4-dinitrotoluene, 2,4,6-trinitrotoluene, and *p*-nitrobenzene). Factors influencing their separation and detection processes were examined and optimised. The four analytes have been well-separated within 120 s in a 75 cm long separation channel at a separation voltage of +2000 V using an electrophoretic separation medium containing 15 mM borax and 15 mM sodium dodecyl sulfate (pH 9.2). Highly linear response is obtained for the four analytes over the range of 0–5 ppm with the detection limits ranging from 12 to 52 ppb. The present system demonstrated long-term stability and reproducibility with relative standard deviations of less than 5% for the peak current ($n = 9$). The new approach for the microchannel–electrode alignment should find a wide range of applications in other microfluidic analysis systems.

Keywords: Miniaturization; Capillary electrophoresis; Amperometric detection; Instrumentation; Nitroaromatic pollutant

1. Introduction

Capillary electrophoresis (CE) microchip systems are of considerable recent interest owing to their high degree of integration, portability, minimal solvent/reagent consumption, high performance, and speed [1–4]. These microchip analysis systems hold considerable promise for environmental monitoring, biomedical, and pharmaceutical analysis, clinical diagnostics, and forensic investigations [5–8]. As with other analysis systems, sensitive detection techniques are highly required for microchip CE. Currently, laser-induced fluorescence (LIF) has dominated the detection for microchip [9]. Mass spectrum (MS) has also received much attention to meet the requirements of proteomic analysis. But, both LIF and MS need rather sophisticated and expensive instrumentations. LIF are limited to fluorescent analytes and analyte derivatives [10]. Recently, electrochemical detection (ECD) has attracted considerable interest for electrophoresis microchip system. It offers great promise for microchip CE systems, with features that include high sensitivity, inherent miniaturization of both the detection and control instrumentations, low-cost, and power demands, and high compatibility with micromaching technology [10–12]. In principle, ECD can be classified into three general modes, conductimetry, potentiometry, and amperometry. However, only conductimetry and amperometry have been commonly used for the detection of microchip CE. Amperometric detection (AD) is the most widely reported ECD method for chip-based separations [10,12–16].

The alignment between the channel outlet and the detection electrode is of high importance because it affects not only the sensitivity but also the reproducibility [11]. The distance between the channel outlet and working electrode also affects the post-capillary band broadening. Two approaches have been employed for the capillary/working electrode arrangements in AD. One is to fabricate the working electrode in or just outside the exit of microchannels. Mathies and co-workers first reported a CE chip with an integrated amperometric detector. They fabricated a band platinum detection electrode just out-

* Corresponding author. Tel.: +86 21 6466 1130; fax: +86 21 6564 1740.
E-mail address: gangchen@fudan.edu.cn (G. Chen).

0039-9140/$ – see front matter © 2006 Elsevier B.V. All rights reserved.
doi:10.1016/j.talanta.2006.01.003

side the exit of separation channel using a photolithographlic process [12]. In this flow-by design, the surface of the band platinum electrode was parallel to the flow direction. Hilmi and Luong [17] described the use of electroless deposition for preparing on-chip gold electrodes. The electroless protocol allows the deposition of the gold film directly onto the channel outlet. This low-cost electroless preparation route obviates the need for photolithographic electrode fabrication or careful channel/electrode alignment. Considering the easy contamination of ampermetric detectors, another approach has been developed to align the detection electrode to the channel outlet with the aid of self-positioning electrode system [18–20]. The separation channel and the detector were divided because such placement of the working electrode results in self-isolation from the high separation potential, owing to the dramatic drop of the potential across the capillary [11]. Such detector allows a fast replacement of passivated electrodes, the comparison and use of different electrode materials, and a convenient surface modification. Wang et al. described a planar screen-printed carbon line electrode for the microchip CE system. The electrode has been no-permanently mounted perpendicular to the channel outlet, allowing easy and fast replacement [18,19]. Cheng and co-workers used a tube fixed on the chip holder to guide the detection electrode to the channel outlet [20]. Unfortunately, neither design allows three-dimensional adjustment. If the carbon line electrodes are not printed in the middle of the support or the position of the guiding tube moves after the epoxy cured, the alignment between the channel outlet and the detection electrode will deteriorate. More recently, a promising end-channel amperometric detector based on a guiding tube for the alignment between the working electrode and the channel outlet was fabricated on glass microchips by different groups [21–23]. The guiding tube, which was in alignment with the outlet of the separation channel, was fabricated directly at the end of the detection reservoir by mechanical drilling [21,22] or chemical etching [23]. Despite these intensive efforts, it is still of high interest to develop a simple and convenient device to simplify the microchannel–electrode alignment procedures.

As an important class of organic compounds, some nitroaromatic compounds are not only explosives, but also toxic environmental pollutants [24]. These compounds can easily enter the soil and water systems from different ways such as the effluent of the chemical and other factories. Development of a simple, rapid, sensitive, and environment-friendly method for different nitroaromatic compound residues is of high interest to environmental land and sea remediation efforts, forensic analysis following terrorist or other criminal activity, and land mine and underwater unexploded ordnance identification for the military. A variety of methods such as gas chromatography (GC) [25,26], high performance liquid chromatography (HPLC) [27,28], immunoassay [29,30], conventional CE [31] and microchip CE [17,32] have been developed for analyzing nitroaromatic compounds. As neutral compounds, nitroaromatic compounds were usually separated by micellar electrokinetic capillary chromatography (MECC) and detected in the reduction mode of amperometric detection.

In this work, a novel microchip CE–AD system been fabricated for the three-dimensional alignment between the separation channel outlet and the detection electrode without a complicated three-dimensional manipulator. This simple and effective system is composed of a CE microchip, a Plexiglas cover plate, a silicon rubber sheet, two screws, a Plexiglas holder containing the amperometric detection reservoir with various electrodes integrated inside. It facilitates not only the fast and easy microchannel–electrode alignment, but also the rapid and simple replacements of electrode and microchip. The fabrication details, feasibility and performance of the high integrated CE–AD system have been demonstrated by separating and detecting nitrobenzene (NB), 2,4-dinitrotoluene (DNT), 2,4,6-trinitrotoluene (TNT) and *p*-nitrobenzene (PNT) in the following sections.

2. Experimental

2.1. Reagent and solutions

Sodium dodecylsulfate (SDS), borax (sodium tetraborate), sodium hydroxide, nitrobenzene (NB), 2,4-dinitrotoluene (DNT) and *p*-nitrobenzene (PNT) were all purchased from Shanghai Chemical Reagent Company (SinoPharm, Shanghai, China) while the stock solution (1000 ppm in acetonitrile) of 2,4,6-trinitrotoluene (TNT) was obtained from Radian International (Austin, TX, USA). All aqueous solutions were made up in doubly distilled water (Medical Center of Fudan University, Shanghai, China). Other chemicals were analytical grade. The electrophoretic buffers were 15 mM borax–15 mM SDS (pH 9.2). Stocking solutions (2000 ppm) of NB, DNT, and PNT were all prepared in absolute ethanol and diluted to the desired concentration with the running buffer just prior to use. The graphite powder was supplied by Aldrich (Wilwaukee, WI, USA).

2.2. Apparatus

Details of the high integrated miniaturized CE–AD system were similar to a previous system [33]. A homemade high voltage power supply had an adjustable voltage range between 0 and +4000 V for the electrophoretic separation and the electrokinetic sample introduction. The glass chip was fabricated by Micralyne (Model MC-BF4-001, Edmonton, Canada) by means of wet chemical etching and thermal bonding techniques. The 86 mm × 16 mm × 2.2 mm chip shown in Fig. 1 consisted of a four-way injection cross with 75 mm long separation channel and side arms of 5 mm long each. The original waste reservoir was cut off; leaving the channel outlet at the end side of the chip, thus facilitate the end-column AD [32]. The channels were 50 μm wide and 20 μm deep. An YS73-4A-3KVA alternate constant-voltage power supply (Shanghai Keyi Instrumental Factory, Shanghai, China) was employed to suppress the voltage fluctuation of the power line. In order to improve the repeatability of the peak current and migration time, the whole CE system was assembled in a room that was air-conditioned at 25 °C to reduce the temperature fluctuation.

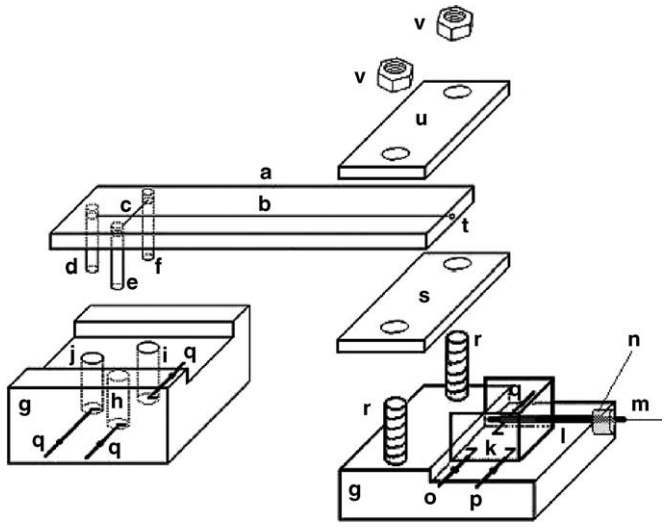

Fig. 1. Schematic diagrams of a three-dimensionally adjustable device for the amperometric detection of microchip capillary electrophoresis. (a) Glass microchip, (b) separation channel, (c) injection channel, (d) pipette tip for buffer reservoir, (e) pipette tip for reservoir not used, (f) pipette tip for sample reservoir, (g) Plexiglas holders, (h) buffer reservoir not used, (i) sample reservoir, (j) buffer reservoir, (k) detection reservoir, (l) stainless-steel guiding tube, (m) capillary-based disc detection electrode, (n) silicon rubber holder, (o) auxiliary electrode, (p) reference electrode, (q) high voltage power electrodes, (r) screw bolts, (s) silicon rubber sheet, (t) channel outlet, (u) Plexiglas cover plate, (v) screw nuts. Dimensions are not in scale.

2.3. Microchip CE–AD system with three-dimensional alignment capability

Details of the three-dimensionally adjustable microchip CE–AD system were illustrated in Fig. 1. Plexiglas holders (g) were fabricated for housing the separation chip (a) and the detection reservoir (k) allowing their convenient replacement and reproducible positioning, with silicone grease providing proper sealing. A three-electrode amperometric detection system was fabricated in the detection reservoir (at the channel outlet side, see Fig. 1) and consisted of a platinum wire auxiliary (o), an Ag/AgCl wire reference (p), and a 320 μm diameter carbon disc detection (m) electrode. The detection electrode (m) was placed opposite the channel outlet (t) through the stainless-steel guiding tube (l, 500 μm i.d. × 800 μm o.d.). Short pipette tips (d–f) was inserted into each of the three holes on the glass chip for solution contact between the channel on the chip and corresponding reservoir (h–j) on the left chip holder in Fig. 1. Platinum wires (q), inserted into the individual reservoirs (h–k), served as contacts to the high voltage power supply. The end of the guiding tube (l) outside the detection reservoir (k) was sealed by a piece of small silicon-rubber holder (n, 3 mm diameter, 2.5 mm thick) with the capillary-based detection electrode (m) inserted inside. The silicon rubber holder (n) could not only prevent solutions in the detection reservoir (k) from leaking, but also hold the detection electrode (m) while allowing the detection electrode to move back and forth to define a desired gap distance to the channel outlet (t). The distance (20 mm) between the two screw bolts (r) on the right Plexiglas holder in Fig. 1 is wider than the width of the microchip (a, 16 mm), allowing the microchip (a) to move right and left slightly to accomplish a good alignment with the detection electrode. A piece of 2.5 mm thick high elasticity silicon rubber sheet (s) was attached to the bottom of the microchip and subsequently sandwiched between a Plexiglas cover plate (u) and the Plexiglas holder (g) with the aid of the screw bolts (r) and screw nut (v), allowing the microchip to be adjusted up and down within approximately 1 mm to align the channel outlet to the detection electrode. With the aids of the two-dimensionally adjustable CE microchip (a) and the one-dimensionally adjustable disc detection electrode (m), the present microchip CE–AD system shown in Fig. 1 facilitates the three-dimensional alignment between the channel outlet and the detection electrode without need of a complicated three-dimensional manipulator.

2.4. Electrode fabrication

A piece of copper wire (10 cm long, 150 μm diameter) was inserted into a 3.0 cm long fused silica capillary (320 μm i.d. × 450 μm o.d., Hebei Yongnian Ruipu Chromatogram Equipment Co., Ltd., Hebei, China) and a 2 mm opening was left in the capillary for the subsequent filling of the graphite–epoxy composite. The other end of the capillary was sealed together with copper wire by thermal adhesive. Epoxy resin and hardener (Zhejian Cixi Tiandong Adhesive Co. Ltd., Ningbo, China) was mixed thoroughly at a weight ratio of 2:1. The graphite powder and epoxy resin/hardener were hand-mixed in a ratio of 1:1 (w/w). The graphite–epoxy composite was subsequently packed into the capillary by pressing the opening end of the capillary (to a depth of ∼3 mm) into a sample of the composite. The graphite–epoxy composite should touch the end of the copper wire inside the capillary tightly for the electric contact. The composite was then allowed to cure at room temperature for at least 3 h.

2.5. End-column amperometric detection

Before use, the microdisc electrode was successively polished with emery paper and alumina powder, sonicated in doubly distilled water, and finally the surface of the detection electrode (Fig. 1(m)) was positioned carefully opposite the channel outlet (Fig. 1(t)) of the separation channel through the guiding metal tube (Fig. 1(l)). The gap distance between the disc electrode and the channel outlet was adjusted to 50 μm approximately by comparison with the channel width (50 μm) while being viewed under a microscope [34,35]. Electrochemical analyzer (CHI 830B, Shanghai Chen-Hua Instruments Co., Ltd., Shanghai, China) was used to provide a constant potential to the detection electrode and measure the output current in combination with the three-electrode electrochemical cell consisting of the laboratory-made disc detection electrode (Fig. 1(m)), the auxiliary electrode (Fig. 1(o)) and the Ag/AgCl wire reference electrode (Fig. 1(p)) using the "amperometric *i–t* curve" mode. The electropherograms were recorded with a time resolution of 0.1 s (without any software filtration) while applying the detection potential. Sample injections were performed after

stabilization of the baseline. All experiments were performed at room temperature.

2.6. Sample preparation

The river water was sampled from Huangpu River at Shanghai (China) and was successively filtered with a filter paper and a polypropylene filter (0.22 μm, Shanghai Bandao Industry Co., Ltd., Shanghai, China). In order to minimize the differences between the water sample and the electrophoretic separation medium (15 mM borax–15 mM SDS), an appropriate amount of borax and SDS was dissolved in the water sample to reach the final concentration of 15 mM, respectively. The sample solution obtained was directly injected for the microchip-CE analysis before and after it was spiked with an appropriate amount of NB, DNT, TNT, and PNT.

2.7. Electrophoretic procedure

The channels of the glass chip were treated before use by rinsing with 0.1 M NaOH aqueous solution and doubly distilled water for 10 min each. The running buffer (Fig. 1(j)) and unused (Fig. 1(h)) reservoirs were filled with electrophoresis running buffer solution, while the sample reservoir (Fig. 1(i)) was filled with a mixture of NB, DNT, TNT, and PNT. The detection reservoir (Fig. 1(k)) was filled with the run buffer solution. In this work, floated injection was employed to introduce the sample solution into the separation channel (Fig. 1(b)). A voltage of +2000 V was applied for 20 s to the sample reservoir (Fig. 1(i)) to facilitate the filling of the injection channel (Fig. 1(c)), while the detection reservoir (Fig. 1(k)) was grounded and all the other reservoirs floating. The sample solution was loaded into the separation channel by applying +2000 V to the sample reservoir (Fig. 1(i)) for 2 or 3 s, while the detection reservoir (Fig. 1(k)) grounded and other reservoirs floating. The separation was usually performed by applying +2000 V to the run buffer reservoir (Fig. 1(j)) with the detection reservoir grounded and other reservoirs floating.

3. Results and discussion

The high precision alignment between the channel outlet and the detection electrode is highly demanded for the microchip CE. In this work, a novel microchip CE–AD system has been fabricated by integrating a two-dimensionally adjustable CE microchip (Fig. 1(a)) and a one-dimensionally adjustable disc detection electrode (Fig. 1(m)) in the Plexiglas holder (Fig. 1(g)) to realize the three-dimensional alignment between the channel outlet (Fig. 1(t)) and the detection electrode with no need of a three-dimensional manipulator. Wang et al. [18,19] have developed a self-positioning AD system for microchip CE by using a planar screen-printed carbon line electrode, while a tube glued on the chip holder has been employed by Cheng and coworkers [20] to guide the detection electrode to the channel outlet. However, both self-aligning detection systems cannot be three-dimensionally adjusted.

The detection electrode is inserted into the detection reservoir (Fig. 1(k)) via the guiding tube (Fig. 1(l)) and the silicone rubber holder (Fig. 1(n)) and can move back and forth, while the specially designed holder allows the right-and-left and up-and-down movements of the microchip with the aid of two screws (Fig. 1(r and v)) and the silicon rubber sheet (Fig. 1(s)) under the microchip to realize the three-dimensional alignment. The silicon rubber holder with a self-sealing bore at its center cannot only immobilize the detection electrode in the guiding tube (Fig. 1(l)), but also make it possible to leave an effective gap distance (usually 30–60 μm) by pushing the detection electrode gently to the chip end until a soft contact is attained due to the native elasticity of rubber. The silicon rubber sheet cannot only allows the up-and-down adjustment of the microchip, but also offers a good sealing between the microchip and the chip holder.

To acquire a good alignment, the cover plate (Fig. 1(u)), the microchip (Fig. 1(a)), the silicon rubber sheet (Fig. 1(s)), and the detection electrode (Fig. 1(m)) are assembled on the holder as shown in Fig. 1. The channel-outlet side of the microchip and the silicon rubber sheet (Fig. 1(s)) should closely touch the side of the detection reservoir so that the gap could be well-sealed with silicone grease to prevent the solution leakage. Although the channel outlet (Fig. 1(t)) could not be seen clearly, the alignment between the microchannel outlet and the detection electrode (Fig. 1(m)) was realized on the basis of the visible separation channel (Fig. 1(b)) and the boundary between the two plates of the microchip with the aid of a microscope. Before fastening the screws (Fig. 1(r and v)), the microchip (Fig. 1(a)) was adjusted to obtain a right-and-left alignment between the microchannel and the detection electrode. And then, the screws were fastened to press the microchip down until the channel outlet directly exposes to the surface of the detection electrode. Finally, the detection electrode was moved back and forth slightly to reach a desired gap distance (for example, 50 μm) to the channel outlet by comparison with the channel width (50 μm) under the microscope. The present system facilitates rapid and easy alignment between the channel outlet and detection electrode without a three-dimensional micromanipulator. It is characterized by its advantages of simple design and construction, ease to operate, reduced alignment time, and low-cost. The noises from mechanical vibration and some other external movements that will disturb the microchannel–electrode alignment are eliminated because the detection electrode and the microchip are both immobilized in the same holder (Fig. 1(g)) with the aids of the elastic silicon rubber holder and sheet (Fig. 1(n and s)). This will lower the noise level so that the sensitivity and stability of the electrochemical detection are improved. In addition, good microchannel–electrode alignment can be easily achieved in a wall-jet configuration because the channel width to the diameter of the disc working electrode is at a ratio of ∼1:6.

Fig. 2 shows the electropherograms for a mixtures containing 20 ppm NB (a), 10 ppm DNT (b), 10 ppm TNT (c), and 20 ppm PNT (d) at the separation voltages of (A) +1000 V, (B) +1500 V, (C) +2000 V, (D) +2500 V, (E) +3000 V, and (F) +3500 V. As expected, increasing the separation voltage from +1000 to +3500 V (A–F) dramatically decreases the migration time, from 170.4 to 48.5, from 182.7 to 52.9, from 203.9 to

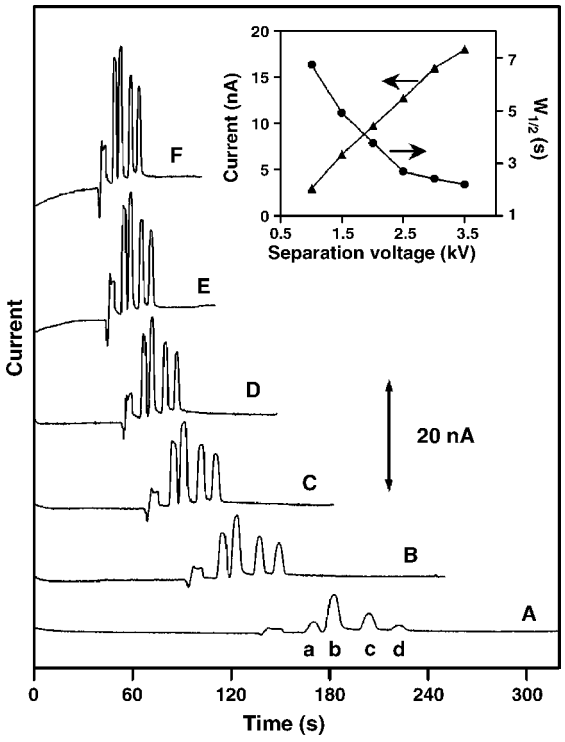

Fig. 2. Electropherograms for a mixtures containing 20 ppm nitrobenzene (a), 10 ppm 2,4-dinitrotoluene (b), 10 ppm 2,4,6-trinitrotoluene (c), and 20 ppm *p*-nitrobenzene (d) at the separation of voltage of (A) +1000, (B) +1500, (C) +2000, (D) +2500, (E) +3000, and (F) +3500 V. Also shown (in the inset) are the resulting plots of the peak current and half peak width ($W_{1/2}$) of 2,4,6-trinitrotoluene (c) upon the separation voltage. Operation conditions: injection voltage, +2000 V; injection time, 3 s; electrophoretic separation medium, 15 mM borax–15 mm SDS (pH 9.2); detection electrode, 320 μm diameter carbon disc electrode; detection potential, −0.65 V (vs. Ag/AgCl wire).

58.8, and from 222.7 to 63.8 s for NB, DNT, TNT, and PNT, respectively. Also shown (in the inset) are the resulting plots of the peak current and half peak width ($W_{1/2}$) of TNT (c) upon the separation voltage. The current response for the reduction of TNT increases in a nearly linear fashion with the increase of separation voltage, indicating that the actual working potential shifted negatively upon raising the separation voltage. The increase of the signal can be ascribed to not only the shift of detection potential, but also the decrease in the migration time and peak width. In addition, the half peak width of NB (a), DNT (b), TNT (c), PNT (d) decreases from 6.4, 6.9, 6.7 and 6.1 s to 2.1, 2.2, 2.2 and 2.1 s, respectively.

Note also that flat baselines and low noise levels are maintained even at high separation voltages. Such a behavior indicates an effective isolation from the high separation voltage. Moreover, higher separation voltages may result in higher Joule heat that directly affects the separation efficiency of this method. However, too lower separation voltages will increase the analysis time considerably, which in turn cause peak broadening. Based on experiments, +2000 was chosen as the optimum separation voltage to accomplish a good compromise.

The detection potential affected not only the peak heights, but also the background current. Hydrodynamic voltammograms (HDVs) of 20 ppm NB, 10 ppm DNT, 10 ppm TNT, and 20 ppm

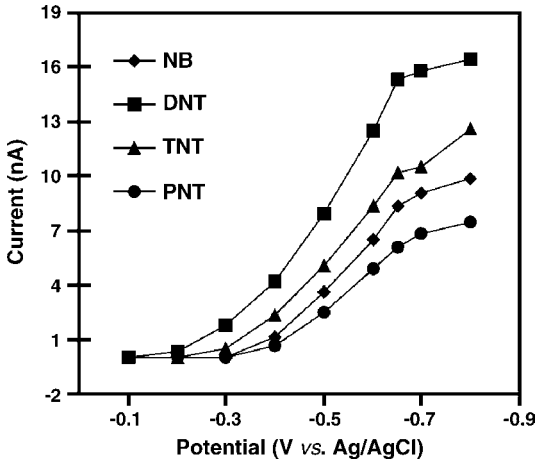

Fig. 3. Hydrodynamic voltammograms for 20 ppm nitrobenzene, 10 ppm 2,4-dinitrotoluene, 10 ppm 2,4,6-trinitrotoluene, and 20 ppm *p*-nitrobenzene on the carbon disc detection electrode. Separation voltage, +2000 V. Other conditions as in Fig. 2.

PNT are illustrated in Fig. 3. The curves were plotted pointwise over the potential range of −0.1 to −0.8 V by changing the applied potential by 0.1 V. The half-wave potential ($E_{1/2}$) values for the reduction of NB, DNT, TNT, and PNT are found to be −0.54, −0.47 −0.50, and −0.55 V (versus Ag/AgCl wire), respectively. All the four analytes display similar profiles, with a rapid increase of the cathodic response starting at −0.40 V. Their peak current increases much slower upon decreasing the potential below −0.65 V. Although an applied potential lower than −0.65 V (versus Ag/AgCl wire) resulted in higher peak currents, the background current increased substantially, resulting in an unstable baseline. The applied potential of the detection electrode was, therefore, maintained at −0.65 V (versus Ag/AgCl wire), under which condition the background current was not too high and the S/N ratio was the highest. At the optimum potential, the detection electrode showed good stability and the reproducibility was high.

The present microchip CE–AD system offers a well-defined concentration dependence. Electropherograms for mixtures containing increasing levels of NB (a), DNT (b), TNT (c), and PNT (d) in increments of 0.5 ppm (for (b) and (c)) and 1 ppm (for (a) and (d)) on a graphite–epoxy composite disc electrode are shown in Fig. 4(A–E). Defined peaks, proportional to the concentration of the four analytes are observed. The resulting calibration plots (shown as inset) are highly linear with sensitivities of 1.02, 2.56, 1.50, and 0.571 nA/ppm for NB (a), DNT (b), TNT (c), and PNT (d) with the corresponding correlation coefficients of 0.9992, 0.9996, 0.9997, and 0.9991, respectively. Detection limits of 29 ppb NB (a), 12 ppb DNT (b), 20 ppb TNT (c), and 52 ppb PNT (d) were estimated on the basis of a single-to-noise ratio of 3, indicating the favorable signal-to-noise characteristics of the detection system. Such values are much better than the detection limits obtained (0.45–0.8 ppm) using a screen-printed carbon line electrode [32].

Good precision is another attractive feature of the new microchip protocol. The precision was examined from a series of nine repetitive injections of a sample mixture containing 10 ppm

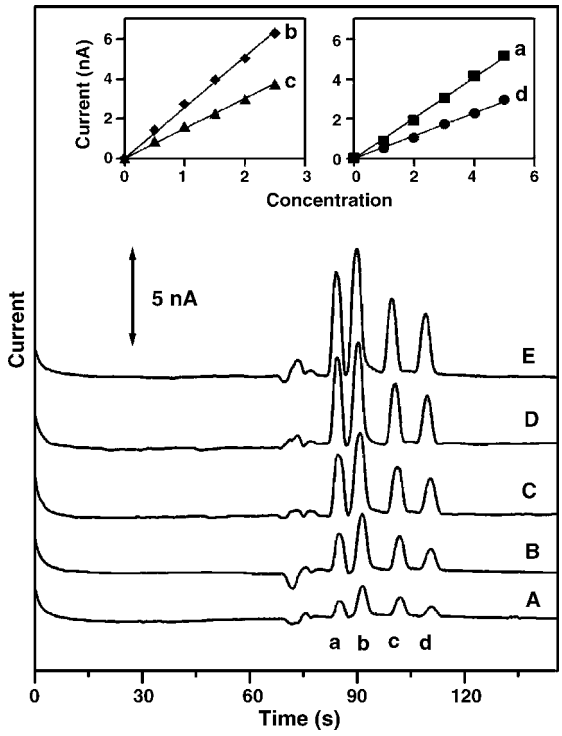

Fig. 4. Electropherograms for mixtures containing increasing levels of NB (a), DNT (b), TNT (c), and PNT (d) in increments of 0.5 ppm (for (b) and (c)) and 1 ppm μM (for (a) and (d)). Also shown (in the insets) are the resulting calibration plots. Separation voltage, +2000 V; injection time, 2 s; other conditions as in Fig. 2.

NB, DNT, TNT, and PNT (conditions as in Fig. 4). Reproducible signals were obtained with relative standard derivation (R.S.D.) of 3.6% (NB), 1.0% (DNT), 1.2% (TNT), and 4.2% (PNT) for the peak currents. Such a good repeatability reflects the stability of the three-dimensionally adjustable microchip CE–AD system and the reduced surface fouling of the carbon electrode and the separation channel, indicating that this approach is suitable for the analyses of real samples.

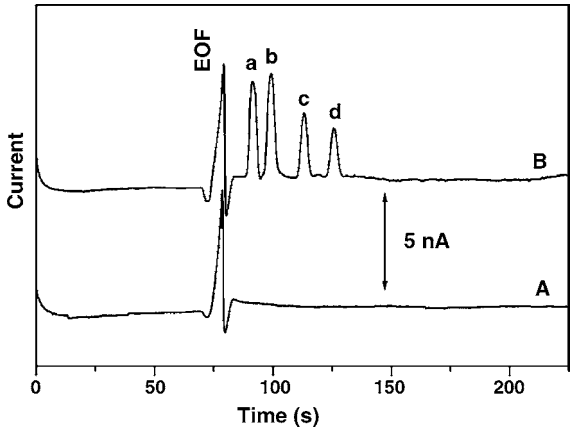

Fig. 5. Electropherograms for a river water sample before (A) and after (B) the addition of 5 ppm NB (a), 2.5 ppm DNT (b), 2.5 ppm TNT (c), and 5 ppm PNT (d). Separation voltage, +2000 V; injection time, 2 s; other conditions as in Fig. 2.

The suitability of the CE microchip for measuring low levels of nitroaromatic pollutants in relevant environmental samples is demonstrated in Fig. 5. The electropherogram for a river water sample, spiked with 5 ppm NB (a), 2.5 ppm DNT (b), 2.5 ppm TNT (c), and 5 ppm PNT (d) is characterized with four well-defined and baseline resolved peaks. As shown in Fig. 5(A), none of the investigated four nitroaromatic pollutants have had been found in the river water. The standard-spiked river water was analyzed under the optimum conditions (Fig. 5(B)). The average recoveries and R.S.D. were 99.2 and 2.4% for NB (a), 95.9 and 1.6% for DNT (b), 97.3 and 3.2% for TNT (c), and 96.4 and 2.9% for PNT (d), respectively ($n = 3$). The results demonstrated that this method had both high accuracy and good precision for the analytes tested in the real sample.

4. Conclusions

The utility and the advantages of the new microchip CE–AD system have been demonstrated by separating and detecting four nitroaromatic pollutants. This system facilitates a high precision and stable three-dimensional alignment between the channel outlet and the detection electrode and has been employed for the analyses of the four analytes in water under the acquired conditions with satisfactory results. The advantages of the present set-up are its simple design and construction, low-cost, high degree of integration, portability, ease to operate, high performance, and speed. The new approach for the three-dimensional microchannel–electrode alignment employed in this work should find more applications in CE, flowing injection analysis, and other microfludic analysis systems.

Acknowledgments

This work was supported by Shanghai Science Committee (051107089 and 2004ZR140150212), NSFC (20405002), and State Education Ministry of China.

References

[1] D. Figeys, D. Pinto, Anal. Chem. 71 (2000) 330A–335A.
[2] D.R. Reyes, D. Iossifidis, P.A. Auroux, A. Manz, Anal. Chem. 74 (2002) 2623–2636.
[3] J. Wang, Electrophoresis 23 (2002) 713–718.
[4] M. Pumera, Talanta 66 (2005) 1048–1062.
[5] W. Chang, Y. Ono, M. Kumemura, T. Korenaga, Talanta 67 (2005) 646–650.
[6] W. Siangproh, O. Chailapakul, R. Laocharoensuk, J. Wang, Talanta 67 (2005) 903–907.
[7] T. Zhang, Q. Fang, S.L. Wang, L.F. Qin, P. Wang, Z.Y. Wu, Z.L. Fang, Talanta 68 (2005) 19–24.
[8] J.Z. Kang, J.L. Yan, J.F. Liu, H.B. Qiu, X.B. Yin, X.R. Yang, E.K. Wang, Talanta 66 (2005) 1018–1024.
[9] V. Dolnik, S.R. Liu, S. Jovanovich, Electrophoresis 21 (2000) 41–54.
[10] W.R. Vandaveer, S.A. Pasas, R.S. Martin, S.M. Lunte, Electrophoresis 23 (2002) 3667–3677.
[11] J. Wang, Talanta 56 (2002) 223–231.
[12] N.A. Lacher, K.E. Garrison, R.S. Martin, S.M. Lunte, Electrophoresis 2 (2001) 2526–2536.
[13] R.S. Martin, K.L. Ratzlaff, B.H. Huynh, S.M. Lunte, Anal. Chem. 74 (2002) 1136–1143.

[14] W.R. Vandaveer IV, S.A. Pasas-Farmer, D.J. Fischer, C.N. Frankenfeld, S.M. Lunte, Electrophoresis 25 (2004) 3528–3549.
[15] L. Nyholm, Analyst 130 (2005) 599–605.
[16] J. Wang, Electroanalysis 17 (2005) 1133–1140.
[17] A. Hilmi, J.H.T. Luong, Anal. Chem. 72 (2000) 4677–4682.
[18] J. Wang, B. Tian, E. Sahlin, Anal. Chem. 71 (1999) 5436–5440.
[19] J. Wang, M.P. Chatrathi, B. Tian, Anal. Chem. 72 (2000) 5774–5778.
[20] Y. Zeng, H. Chen, D.W. Pang, Z.L. Wang, J.K. Cheng, Anal. Chem. 74 (2002) 2441–2445.
[21] Y.R. Wang, H.W. Chen, J. Chromatogr. A 1080 (2005) 192–198.
[22] F. Meng, H.W. Chen, Y.H. Dou, Z.L. Fang, Chem. J. Chinese Univ. 25 (2004) 844–846.
[23] Y.Y. Wu, J.M. Lin, R.G. Su, F. Qu, Z.W. Cai, Talanta 64 (2004) 338–344.
[24] G. Chen, Y.H. Lin, J. Wang, Talanta 68 (2006) 497–503.
[25] M. Hable, C. Stern, C. Asowata, K. Williams, J. Chromatogr. Sci. 29 (1991) 131–136.
[26] J.M. Perr, K.G. Furton, J.R. Almirall, Talanta 67 (2005) 430–436.
[27] W. Kleibohmer, K. Camman, J. Robert, E. Musenbrock, J. Chromatogr. 638 (1993) 349–356.
[28] R.L. Marple, W.R. LaCourse, Talanta 66 (2005) 581–590.
[29] M. Kobayashi, M. Sato, Y. Li, N. Soh, K. Nakano, K. Toko, N. Miura, K. Matsumoto, A. Hemmi, Y. Asano, T. Imato, Talanta 68 (2005) 198–206.
[30] K. Matsumoto, A. Torimaru, S. Ishitobi, T. Sakai, H. Ishikawa, K. Toko, N. Miura, T. Imato, Talanta 68 (2005) 305–311.
[31] A. Hilmi, J.H.T. Luong, A.L. Nguyen, Anal. Chem. 71 (1999) 873–878.
[32] G. Chen, J. Wang, Analyst 129 (2004) 507–511.
[33] G. Chen, L.Y. Zhang, J. Wang, Talanta 64 (2004) 1018–1023.
[34] G. Chen, J.X. Zhang, X.L. Wu, Microchim. Acta 148 (2004) 143–150.
[35] G.X. Xu, J. Wang, Y. Chen, L.Y. Zhang, D.R. Wang, G. Chen, Lab Chip 6 (2006) 145–148.